



Published in final edited form as:

Jpn J Ophthalmol. 2016 September ; 60(5): 408–418. doi:10.1007/s10384-016-0461-1.

The role of Prdx6 in the protection of cells of the crystalline lens from oxidative stress induced by UV exposure

Shinsuke Shibata¹, Naoko Shibata¹, Teppei Shibata¹, Hiroshi Sasaki¹, Dharendra P. Singh², and Eri Kubo¹

¹Department of Ophthalmology, Kanazawa Medical University, 1-1 Daigaku, Uchinada, Kahoku, Ishikawa 920-0293, Japan

²Department of Ophthalmology and Visual Sciences, University of Nebraska Medical Center, Omaha, USA

Abstract

Purpose—The immediate aim of this study was to investigate alterations in peroxiredoxin (Prdx) 6 at posttranslational levels, and the levels of protein oxidation, lipid peroxidation, and reactive oxygen species (ROS) in lens epithelial cells (LECs) after exposure to severe oxidative stress, such as ultraviolet-B (UV-B). Our ultimate aim was to provide new information on antioxidant defenses in the lens and their regulation, thereby broadening existing knowledge of the role of Prdx6 in lens physiology and pathophysiology.

Methods—The expression of the hyperoxidized form of Prdx6 and oxidation of protein were analyzed by western blotting and the OxyBlot assay in human LECs (hLECs). ROS levels were quantified using DCFH-DA dye, and cell viability was quantified by the MTS and TUNEL assays. To evaluate the protective effect of Prdx6, we cultured lenses with or without the TAT transduction domain (TAT-HA-Prdx6) and observed (and photographed) the cultures at specified time-points after the exposure to UV-B for the development of opacity.

Results—Prdx6 in hLECs was hyperoxidized after exposure to high amounts of UV-B. UV-B treatment of hLECs increased the levels of cell death, protein oxidation, and ROS. hLECs exposed to UV-B showed higher levels of ROS, which could be reduced by the application of extrinsic TAT-HA-Prdx6, attenuating UV-B-induced lens opacity and apoptotic cell death.

Conclusion—Excessive oxidative stress induces the hyperoxidation of Prdx6 and may reduce the ability of Prdx6 to protect LECs against ROS or stresses. Because extrinsic Prdx6 could attenuate UV-B-induced abuse, this molecule may have a potential in preventing cataractogenesis.

Keywords

Cataract; Lens epithelial cells; Oxidative stress; Peroxiredoxin 6; Ultraviolet-B

Correspondence to: Eri Kubo.

Conflicts of interest S. Shibata, None; N. Shibata, None; T. Shibata, None; H. Sasaki, None; D. P. Singh, None; E. Kubo, None.

Introduction

Age-related cataract is a multifactorial condition, the incidence and progression of which are modified by age, sex, and exposure to ultraviolet (UV) radiation and X-rays, oxidation, and biomolecules such as transforming growth factor beta and tumor necrosis factor alpha (TNF- α) [1–3]. The most significant factor in the lenticular cells of eyes maximally exposed to environmental stress is oxidative load [4]. To cope with oxidative stress, the crystalline lens has evolved antioxidant defense systems, including antioxidant enzymes of varying capacity, such as superoxide dismutase, selenium-dependent glutathione (GSH) peroxidase, catalase, glutathione-S-transferase, and the recently defined rapidly growing family of peroxiredoxins (Prdxs) [5–7]. During cataractogenesis, oxidative stresses induce injurious events, resulting in posttranslational modifications of lens' proteins, leading to their aggregation, fragmentation, and precipitation, which in turn causes lens opacification. Furthermore, exposure of the eye to UV-B (290–315 nm) can cause cortical and posterior subcapsular cataracts in humans and animals [8–13]. UV irradiation of the lens induces active oxygen species (ROS), including hydrogen peroxide (H₂O₂) and superoxide ions [14–16]. Increased ROS-driven oxidative stress generates various aberrant cellular responses, including damage to DNA and proteins [10], hyperactivation of signal transduction pathways [17, 18], and activation/deactivation of gene expression [19, 20].

The Prdxs, a family of antioxidants, provide cytoprotection against internal/external environmental stresses by clearing the oxidative load [21, 22]. The mammalian Prdx family constitutes six members (Prdx1 to -6) [21, 23–25]. All Prdxs have two catalytically active cysteines—with the exception of Prdx6, a cytosolic antioxidant, which contains only one conserved cysteine, C47 [21, 23–25]. C47 is necessary for the GSH peroxidase activity of Prdx6. Moreover, this protein is more highly expressed in murine lenses than are the other members of the Prdx family [7]. Prdx6 expression is upregulated in lens epithelial cells (LECs) exposed to UV-B, dexamethasone, or TNF- α . In the mice model, expression of Prdx6 in the murine lens increases after birth, peaks at 6 months, and decreases with age [7]. During the prenatal period, Prdx6 is localized in the primary lens fibers and LECs; after birth and during aging, however, Prdx6 localizes to the surface cortical fibers (secondary differentiated fibers). This localization pattern reflects its biologic functions, which are associated with its antioxidant properties and possibly a role in cellular signaling [7].

Prdx6 is a multifunctional protein. Its mRNA has been cloned and expressed from a human LEC (hLEC) cDNA library [5]. It has unique protective function(s) that are nonreductant to those of other antioxidants and involved in cytoprotection against various external and internal stressors [5, 6, 26–33]. The encoded protein has been shown to protect hLECs from apoptosis induced by H₂O₂ or hyperglycemia [25, 34]. Although classified as a Prdx on the basis of its homology, the properties of Prdx6 clearly differentiate it from other members of the mammalian Prdx family. Moreover, the sequence associated with Prdx6 activity is not present in other Prdxs [27]. In various studies, Prdx6-depleted (*Prdx6*^{-/-}) murine LECs exhibited elevated expression of ROS, showed spontaneous apoptosis, and were more vulnerable to oxidative stress-induced apoptosis than were LECs expressing Prdx6 [5, 6, 35]. In addition, *Prdx6*^{-/-} murine lenses developed cataracts after exposure to oxidative stress [5].

The catalytic center of Prdx6, as well as of the other Prdxs, consists of cysteine, rather than selenocysteine, which characterizes the glutathione peroxidases [36, 37]. The N-terminus conserved cysteines (Cys51 of Prdx1) of Prdx1 to -5 are selectively oxidized by H₂O₂ to Cys-SOH [38], which, in turn, reacts with the Cys172-SH of another Prdx molecule, creating a homodimer through an intermolecular disulfide bond (Fig. 1). The disulfide is subsequently reduced to the Prdx active thiol form by the thioredoxin–thioredoxin reductase system [39–44]. Under oxidative stress conditions, however, the sulfenic intermediate is susceptible to hyperoxidation and may be hyperoxidized by H₂O₂, leading to the formation of sulfinic (Cys-SO₂H) or sulfonic (Cys-SO₃H) acid, which cannot form disulfide bonds with the resolving cysteine [36, 44, 45]. Furthermore, at high concentrations of H₂O₂ (>100 μM), Prdx6 and 2-Cys Prdxs are hyperoxidized. In contrast to the hyperoxidation of 2-Cys Prdxs, the hyper-oxidation of Prdx6 is irreversible in vivo [46] (Fig. 1). Overoxidation of the catalytical cysteine, whether by H₂O₂ or by cell cycle-dependent phosphorylation, can inactivate the Prdxs. Oxidative modification of Prdx6 may therefore act as a sensor of oxidative load, triggering signal transduction to counter oxidative stress.

We previously reported an association between Prdx6 expression in human cataractous lenses and age: older patients (aged >70 years) showed significantly lower expression of Prdx6 mRNA than did relatively younger patients (aged <70 years) [47]. In addition, the expression of Prdx6 mRNA was significantly lower in lenses with relatively more severe nuclear and cortical cataracts in patients aged <70 years [47]. Based on the results of this study, we speculated that the decreased expression of Prdx6 mRNA may induce oxidative stress in human lenses, leading in turn to age-related cataracts.

In the study reported here, we investigated the oxidative regulation of Prdx6, including alterations at the posttranslational level, and observed that ROS-driven oxidative stress induced by exposure to UV-B was associated with protein oxidation in LECs. Addition of the extrinsic Prdx6-linked transactivating transduction (TAT) domain reversed oxidative stress-mediated apoptosis processes by clearing the oxidative load as well as ablating oxidative stress-induced lens opacity in lens organ culture. These findings provide new information on antioxidant defenses in the lens and their regulation, thereby enhancing knowledge of the role of Prdx6 in lens physiology and pathophysiology.

Methods

Prokaryotic expression of recombinant Prdx6 protein

The human immunodeficiency virus (HIV)-TAT domain has 11 amino acids (RKKRRQRRR) and can deliver 100 % of proteins across the plasma membrane and the blood–brain barrier [6, 48–51]. In this study, we used the ability of the TAT domain to infiltrate cells and constructed a recombinant TAT-linked Prdx6 protein. Briefly, full-length Prdx6 cDNA was cloned into a TA-cloning vector (Invitrogen/Thermo Fisher Scientific, Waltham, MA), which was used to transform competent prokaryotic cells. Plasmids of selected colonies were purified, and the purified TA vector containing Prdx6 cDNA was subcloned into a pTAT-HA expression vector (a kind gift of Dr. S.F. Dowdy). The expressed recombinant protein TAT-HA-Prdx6 was purified on a Ni²⁺-nitrilotriacetic acid Sepharose column (Invitrogen). The negative controls included mutated TAT-linked Prdx6 protein, in

which the cysteine residue at amino acid 47 of the redox-active functional site was replaced by an isoleucine residue.

Cell culture

Simian virus 40-transformed hLECs (SRA01/04) (a kind gift of Dr. N. Ibaraki of the Ibaraki Eye Clinic, Tochigi, Japan) were cultured in Dulbecco's modified Eagle's medium (DMEM; Wako, Osaka, Japan) containing 20 % fetal bovine serum (FBS; Sigma, St. Louis, MO) to 80 % confluence at 37 °C in an air-CO₂ (19:1) atmosphere for 24 h. For the UV-B irradiation assays, the hLECs were placed in 1 mL of 1× phosphate-buffered saline (PBS), irradiated with 0, 2.0, or 8.0 kJ/m² UV-B, and thereafter changed to fresh medium containing 2 % FBS. UV-B light was generated by a 15-W UV-B light source (312 nm), with its intensity standardized using a UV light meter (UVP, Upland, CA).

Assay for intracellular redox state and cell viability

Intracellular redox levels were measured using the fluorescent dye 2,7-dichlorofluorescein diacetate (DCFH-DA) (Cell Biolabs, San Diego, CA), a nonpolar compound that is converted into a polar derivative (DCFH) by cellular esterases after incorporation into cells. For the UV-B irradiation assays, hLECs were cultured in DMEM supplemented with 2 % FBS in 96-well chamber slides (Nalge Nunc, Rochester, NY) after irradiation with 0.0, 2.0, or 8.0 kJ/m² UV-B. The medium was replaced with Hank's solution containing 10 μM DCFH-DA (Cayman Chemical, Ann Arbor, MI) and incubated for 10 min at room temperature. Intracellular fluorescence was detected at an excitation wavelength of 485 nm and an emission wavelength of 530 nm using Spectra Max Gemini EM (Molecular Devices, Sunnyvale, CA).

The MTS assay (Promega, Madison, WI) of cellular proliferation/viability uses 3-(4,5-dimethylthiazol-2-yl)-5-(3-carboxymethoxyphenyl)-2 to 4-sulphophenyl) 2H-tetra-zolium salt (MTS). When added to medium containing viable cells, MTS is reduced to a water-soluble formazan salt. The A490-nm value (A = absorbance) was measured after 4 h with a microplate reader (Bio-Rad Laboratories, Hercules, CA). The results were normalized with absorbance of the untreated control(s).

Detection of protein oxidation

Protein oxidation results in the introduction of carbonyl groups into protein side chains by site-specific mechanisms. Carbonyl groups in proteins extracted from UV-B-treated hLECs were detected using a OxyBlot Protein Oxidation Detection kit (Chemicon, Temecula, CA) according to the manufacturer's instructions. Protein samples (10 μg) were treated with 2,4-dinitrophenylhydrazine (DNP-hydrazine) to derivatize the carbonyl groups to 2,4-dinitrophenylhydrazone (DNP-hydrazone) and then electrophoretically separated on 10- to 20 % gradient sodium dodecyl sulfate (SDS)-polyacrylamide gels, followed by transfer to polyvinylidene difluoride membranes (Trans Blot Turbo Transfer Pak; Bio-Rad Laboratories). The membranes were incubated with primary antibody specific to the DNP moiety of the proteins, followed by incubation with horseradish peroxidase-antibody conjugate directed against the primary antibody. Bands were detected using the ECL Western Blotting Detection system (GE Healthcare, Buckinghamshire, UK).

Protein blots

Protein extracts of hLEC were prepared in ice-cold radioimmunoprecipitation buffer, as previously described [7, 52, 53]. Proteins (aliquots of 20 µg) were electrophoretically resolved on 10- to 20 % gradient SDS-polyacrylamide gels, transferred to polyvinylidene difluoride membranes (Bio-Rad), and incubated with anti-mouse Prdx6 monoclonal antibody (Ab) (Abcam, Cambridge, UK) and anti-rabbit-PrdxVI-SO₃ polyclonal Ab (GenWay Biotech, San Diego, CA, USA) to detect the sulfinic and sulfonic forms of Prdx6, respectively, and with anti-β actin monoclonal Ab (Abcam) (dilution, 1:300) as a loading control.

Apoptosis assay

Apoptotic cell death was analyzed by terminal deoxynucleotidyl transferase dUTP-mediated nick-end labeling (TUNEL) assays. TUNEL staining was performed using an in situ cell death detection kit and fluorescein (Roche Diagnostics, Mannheim, Germany), following the manufacturer's protocol. Briefly, cells were washed with PBS, fixed in freshly prepared 4 % paraformaldehyde in PBS (pH 7.4), and incubated in permeabilization solution (0.1 % Triton X-100, 0.1 % sodium citrate) for 2 min on ice. The cells were washed twice with PBS and incubated in a TUNEL reaction mixture for 60 min at 37 °C in the dark. After three washes with PBS, the samples were mounted, viewed by photomicroscopy (ECLIPSE TE 300; Nikon, Tokyo, Japan), and analyzed.

Animals

All animal experiments were approved by the Committee of Animal Research of Kanazawa Medical University and conducted in accordance with the National Institutes of Health Guide for the Care and Use of Laboratory Animals, the recommendations of the ARVO Statement for the Use of Animals in Ophthalmic and Vision Research, and the Institutional Guidelines for Laboratory Animals of Kanazawa Medical University (permission number: 2013–88). Nine female albino Sprague–Dawley rats aged 4 weeks, obtained from Clea Japan (Osaka, Japan), were killed through CO₂ inhalation. Their eyes were removed and the lenses dissected by a posterior approach. Each transparent lens was placed in a well of a 24-well culture plate containing 1.5 mL/well of Medium 199 (Gibco/Thermo Fisher Scientific) for 24 h. The pH was adjusted to 7.2 and the osmolality to 300 ± 5 mOsmol. Organ-cultured transparent lenses were irradiated with UV light set at 0 and 6.0 kJ/m² (*n* = 3 per group). After 120 h, the lenses were photographed by means of a stereomicroscope with dark-field illumination (Stemi DV4; Zeiss, Jena, Germany). The opacity density was analyzed using MultiGauge Software (Fuji Film, Tokyo, Japan).

Statistical analysis

Data were reported as means ± SD for the indicated number of experiments and analyzed by one-way analysis of variance, followed by a *t* test when appropriate. Probability values of 0.05 were defined as significant.

Results

UV-B induced ROS-driven cell death and oxidation of protein in hLECs

Cell viabilities were significantly decreased in hLECs exposed to 2.0 and 8.0 kJ/m² UV-B for 60 min (Fig. 2a). Quantitation of ROS levels using H₂-DCFH-DA assays showed that ROS levels were significantly increased in hLECs exposed to 2.0 kJ/m² UV-B for 60 min and to 8.0 kJ/m² UV-B for 30 and 60 min, respectively (Fig. 2b).

The effect of hyperoxidative load on intracellular protein carbonylation was assessed by the Oxyblot assay. Protein carbonylation can be used as a biomarker of oxidative stress. Because UV-B is a producer of oxidative stress and eyes are maximally exposed to sunlight, we examined whether the exposure of LECs to UV-B radiation would lead to protein oxidation. Oxyblot analysis of cells exposed to variable doses of UV-B radiation for different time periods revealed that oxidative modification of proteins was directly related to the dose and duration of UV-B exposure (Fig. 3). Oxidation of protein was detected in hLECs with a 60-min exposure to 2.0 kJ/m² UV-B and with a 30- and 60-min exposure to 8.0 kJ/m² UV-B (Fig. 3).

UV-B radiation induced expression of hyperoxidized Prdx6 (Prdx6-SO₃) in hLECs

To determine whether Prdx6 is hyperoxidized in cells exposed to UV-B, LECs were exposed to 2.0 and 8.0 kJ/m² UV-B for 10, 30, or 60 min, and cellular extracts were prepared and immunoblotted with anti-Prdx6-SO₃ antibody. Exposure of hLECs to various doses of UV-B radiation showed that treatment for 10 and 30 min with 2.0 kJ/m² UV-B and for 10, 30, and 60 min with 8.0 kJ/m² UV-B significantly increased the hyperoxidation of Prdx6 and the formation of Prdx6-SO₃ in LECs (Fig. 4). Treatment for 60 min with 2.0 kJ/m² UV-B slightly increased the hyperoxidation of Prdx6 and the formation of Prdx6-SO₃ in LECs; however, the total Prdx6 and β-actin levels did not change (Fig. 4).

Exogenous TAT-HA-Prdx6 attenuates UV-B-induced ROS generation in hLECs

TAT-like proteins are efficiently internalized in cells and organs in a concentration-dependent manner and remain biologically active [6, 34, 50, 54, 55]. Although 5–10 μg/mL of TAT-HA-Prdx6 was found to optimally protect many cell types, the concentrations required may vary by cell type and concentration. Because 10 μg/mL TAT-HA-Prdx6 is nontoxic to cells, we assessed its ability to protect LECs from UV-B radiation-induced cellular injuries. Cultured LECs pretreated with 10 μg/mL TAT-HA-Prdx6 were exposed to 2.0 or 8.0 kJ/m² UV-B radiation for 1 and 2 h (Fig. 5a, b). As expected, ROS levels were significantly increased after exposure to 2.0 and 8.0 kJ/m² UV-B of cells pretreated with mutant TAT-HA-Prdx6, in which the active site cysteine 47 was replaced by isoleucine following exposure to UV-B (Fig. 5a, b). In contrast, cells pretreated with exogenous TAT-HA-Prdx6 showed significantly reduced ROS levels 1 and 2 h after exposure to 2.0 kJ/m² UV-B radiation (Fig. 5a). Cells pretreated with exogenous TAT-HA-Prdx6 also showed significantly reduced ROS levels 1 h after exposure to 8.0 kJ/m² UV-B radiation (Fig. 5b). However, exogenous TAT-HA-Prdx6 did not significantly reduce ROS levels 2 h after exposure to 8.0 kJ/m² UV-B radiation (Fig. 5b).

Effect of exogenous TAT-HA-Prdx6 on UV-B-induced apoptosis of hLECs

These findings indicate that UV-B generates a high oxidative load in hLECs and that this increased oxidative load may surpass the threshold level and induce cell death. We therefore assessed whether UV-B radiation induces apoptosis in hLECs and whether this can be inhibited by treatment with exogenous TAT-HA-Prdx6. As our results indicated that cell death was significantly induced after 1 h of exposure to 2.0 kJ/m² UV-B (Fig. 2a), we conducted an apoptosis assay at 1 and 8 h following exposure to 2.0 kJ/m² UV-B for 1 h. The TUNEL assays showed that LECs underwent apoptotic cell death 1 and 8 h after exposure to 2.0 kJ/m² UV-B radiation (Fig. 6a, b). However, the addition of exogenous TAT-HA-Prdx6 (10 and 20 µg/mL) significantly reduced the number of TUNEL-positive cells (Fig. 6a, b) when compared with the addition of mutant Prdx6 (20 µg/mL) 1 and 8 h after 2.0 kJ/m² UV-B radiation. These results suggest that exogenous TAT-HA-Prdx6 prevents UV-B-induced apoptosis in hLECs.

Exogenous TAT-HA-Prdx6 prevents the onset of UV-B-induced cataracts

To determine if exogenous TAT-HA-Prdx6 could abrogate UV-B-induced development of opacity in crystalline lenses cultured in vitro, we treated organ cultures of rat lenses with TAT-HA-Prdx6 or its mutant and exposed the treated cultures to UV-B radiation (Fig. 7a). Lens opacity at 120 h after exposure to 6.0 kJ/m² UV-B irradiation was significantly greater in organ cultures treated with 20 µg/mL of the mutant TAT-HA-Prdx6 (Fig. 7a, upper panel) than in those treated with 10 or 20 µg/mL of TAT-HA-Prdx6 (Fig. 7a, middle and lower panels), indicating that exogenous TAT-HA-Prdx6 significantly reduced the area of opacity (Fig. 7a, b).

Discussion

The results of this study show that exposure of hLECs to oxidative stress induced by UV-B resulted in the hyper-oxidation of Prdx6. Agents of oxidative stress, such as UV light and high glucose, are major factors in the induction of cataractogenesis [35, 56–61]. Consequently, determining the threshold of protein oxidation for lens opacification is of pathogenic importance [62]. In our study, Prdx6 was slightly hyperoxidized at 2.0 kJ/m² UV-B after 10 and 30 min but was rapidly hyperoxidized at 8.0 kJ/m² UV-B after 10–60 min. Prdx6 has been shown to act as a cellular indicator of hyperoxidative stress through the hyperoxidation of the cysteine 47 residue and to play a role in cellular toxicity [46]. In that study, treatment of both HeLa and HEK293 cells with H₂O₂ concentrations of > 100 µM H₂O₂ induced apoptosis—findings which are consistent with Prdx6 hyperoxidation. Under higher than normal H₂O₂ concentrations, however, Prdx6 was rapidly hyperoxidized, increasing its iPLA2 (calcium-independent phospholipase A2) activity and inducing cell cycle arrest, showing that Prdx6 is involved in H₂O₂-induced cellular toxicity [46]. Inactivation of Prdx6 hyperoxidation in lenses may accelerate the generation of ROS and cell death in crystalline lenses.

We previously reported that Prdx6 protects human and murine LECs and bovine retinal pericytes from H₂O₂-, UV-B-, and hyperglycemia-induced apoptosis [5, 6, 34, 35, 57]. The finding of the current study show that the addition of TAT-HA-Prdx6 inhibited the UV-B (2.0

kJ/m^2) induction of ROS and apoptosis in cultured hLECs and of cataracts in organ-cultured rat lenses. However, hyperoxidation of Prdx6 may reduce cellular protection at higher oxidative stress, such as exposure to 8.0 kJ/m^2 UV-B. We found that the addition of TAT-HA-Prdx6 reduced the ROS levels at 1 h—but not at 2 h—after exposure to 8.0 kJ/m^2 UV-B radiation. It is possible that the extrinsic supply of TAT-HA-Prdx6 may inhibit ROS production temporally, whereas excessive and prolonged ROS production after 8.0 kJ/m^2 UV-B exposure may oxidize the supplied TAT-HA-Prdx6 in hLECs that have lost their antioxidative ability.

Irradiation by UV light generates ROS, including H_2O_2 and superoxide ions [16, 63], which in turn induces various cellular responses in eukaryotes, including damage to DNA and proteins [64, 65], triggering of signal transduction pathways [66–68], and activation of gene expression [66, 68–71]. UV-B triggers the apoptotic pathway during irradiation, although the actual apoptotic process occurs later [10]. The combination of oxidative stress and direct damage to DNA and membranes leads to a loss of epithelial cell viability. Ayala et al. showed that UV radiation in organ-cultured lenses induces apoptosis of LECs [72]. During apoptosis, mitochondria in lens cells are under increased oxidative stress, which is considered to be an initiating factor for the onset of cataract development to maturity [59, 73]. We found that the addition of exogenous TAT-HA-Prdx6 protein before UV-B exposure prevented UV-induced apoptosis, DNA damage, and ROS production, and delayed UV-B-induced cataract. The aim of our study was to reveal that TAT-HA-Prdx6 could effectively blunt oxidative load by eliminating ROS and thereby inhibit UV-B induced apoptosis in cultured hLECs. We would like to emphasize that apoptotic events in the epithelium precede, both temporally and spatially, macroscopic cataractogenesis. The use of antioxidants to reduce the harmful effects of UV-B irradiation is a novel approach to photoprotection and cataract prevention.

TAT-HA-Prdx6 is transduced in LECs and lenses and protects LECs from oxidative stress [5, 6]. Moreover, Prdx6 has been shown to prevent oxidative stress-induced pathologic changes in vitro and in vivo. Intracellular delivery of mature proteins for therapeutic purposes has been limited owing to the impermeable nature of plasma membranes. However, the HIV-TAT domain has been shown to have a 100 % potential for intracellular delivery of proteins across the plasma membrane and the blood brain barrier [48–51, 74].

In conclusion, the results of our study provide the first evidence that hyperoxidized Prdx6 is generated by hLECs in response to UV-B exposure. Prdx6 functions both as an antioxidant enzyme and as a cellular indicator of higher oxidative stress. The antioxidant TAT-HA-Prdx6 may be useful for photoprotection and for the prevention of lens opacity and cell death of LECs induced by UV-B.

Acknowledgments

We gratefully acknowledge 3 grants provided by the National Eye Institute (NIH) (EY024589) and Research for Preventing Blindness (RPB) to Singh DP and Japan Society for the Promotion of Science (JSPS) KAKENHI Grant Numbers JP16689027 provided to Kubo E.

References

1. Harding, JJ., Crabbe, MJC. The lens: development, proteins, metabolism and cataract. In: Davson, H., editor. The eye. 3. London: Academic Press; 1984. p. 207-492.
2. McAvoy JW, Chamberlain CG, de Iongh RU, Hales AM, Lovicu FJ. Peter Bishop lecture. Growth factors in lens development and cataract: key roles for fibroblast growth factor and TGF-beta. *Clin Exp Ophthalmol.* 2000; 28:133-9. [PubMed: 10981780]
3. Lovicu FJ, Schulz MW, Hales AM, Vincent LN, Overbeek PA, Chamberlain CG, et al. TGFbeta induces morphological and molecular changes similar to human anterior subcapsular cataract. *Br J Ophthalmol.* 2002; 86:220-6. [PubMed: 11815351]
4. Lou MF. Redox regulation in the lens. *Prog Retin Eye Res.* 2003; 22:657-82. [PubMed: 12892645]
5. Fatma N, Kubo E, Sharma P, Beier DR, Singh DP. Impaired homeostasis and phenotypic abnormalities in Prdx6^{-/-} mice lens epithelial cells by reactive oxygen species: increased expression and activation of TGFbeta. *Cell Death Differ.* 2005; 12:734-50. [PubMed: 15818411]
6. Kubo E, Fatma N, Akagi Y, Beier DR, Singh SP, Singh DP. TAT-mediated PRDX6 protein transduction protects against eye lens epithelial cell death and delays lens opacity. *Am J Physiol Cell Physiol.* 2008; 294:C842-55. [PubMed: 18184874]
7. Kubo E, Miyazawa T, Fatma N, Akagi Y, Singh DP. Development- and age-associated expression pattern of peroxiredoxin 6, and its regulation in murine ocular lens. *Mech Ageing Dev.* 2006; 127:249-56. [PubMed: 16321424]
8. Zigman S, Vaughan T. Near-ultraviolet light effects on the lenses and retinas of mice. *Invest Ophthalmol.* 1974; 13:462-5. [PubMed: 4831699]
9. Taylor HR, West SK, Rosenthal FS, Munoz B, Newland HS, Abbey H, et al. Effect of ultraviolet radiation on cataract formation. *N Engl J Med.* 1988; 319:1429-33. [PubMed: 3185661]
10. Li WC, Spector A. Lens epithelial cell apoptosis is an early event in the development of UV-B-induced cataract. *Free Radic Biol Med.* 1996; 20:301-11. [PubMed: 8720900]
11. Jose JG. Posterior cataract induction by UV-B radiation in albino mice. *Exp Eye Res.* 1986; 42:11-20. [PubMed: 3956601]
12. Bochow TW, West SK, Azar A, Munoz B, Sommer A, Taylor HR. Ultraviolet light exposure and risk of posterior subcapsular cataracts. *Arch Ophthalmol.* 1989; 107:369-72. [PubMed: 2923558]
13. Bachem A. Ophthalmic ultraviolet action spectra. *Am J Ophthalmol.* 1956; 41:969-75. [PubMed: 13327004]
14. Babu V, Misra RB, Joshi PC. Ultraviolet-B effects on ocular tissues. *Biochem Biophys Res Commun.* 1995; 210:417-23. [PubMed: 7755617]
15. Andley UP, Clark BA. Photoreactions of human lens monomeric crystallins. *Biochim Biophys Acta.* 1989; 997:284-91. [PubMed: 2548626]
16. Andley UP, Clark BA. The effects of near-UV radiation on human lens beta-crystallins: protein structural changes and the production of O₂⁻ and H₂O₂. *Photochem Photobiol.* 1989; 50:97-105. [PubMed: 2762385]
17. Wu S, Tan M, Hu Y, Wang JL, Scheuner D, Kaufman RJ. Ultraviolet light activates NFkappaB through translational inhibition of IkappaBalpha synthesis. *J Biol Chem.* 2004; 279:34898-902. [PubMed: 15184376]
18. Wu S, Hu Y, Wang JL, Chatterjee M, Shi Y, Kaufman RJ. Ultraviolet light inhibits translation through activation of the unfolded protein response kinase PERK in the lumen of the endoplasmic reticulum. *J Biol Chem.* 2002; 277:18077-83. [PubMed: 11877419]
19. Oh JH, Chung AS, Steinbrenner H, Sies H, Brenneisen P. Thioredoxin secreted upon ultraviolet A irradiation modulates activities of matrix metalloproteinase-2 and tissue inhibitor of metalloproteinase-2 in human dermal fibroblasts. *Arch Biochem Biophys.* 2004; 423:218-26. [PubMed: 14871484]
20. Afaq F, Malik A, Syed D, Maes D, Matsui MS, Mukhtar H. Pomegranate fruit extract modulates UV-B-mediated phosphorylation of mitogen-activated protein kinases and activation of nuclear factor kappa B in normal human epidermal keratinocytes paragraph sign. *Photochem Photobiol.* 2005; 81:38-45. [PubMed: 15493960]

21. Wood ZA, Poole LB, Karplus PA. Peroxiredoxin evolution and the regulation of hydrogen peroxide signaling. *Science*. 2003; 300:650–3. [PubMed: 12714747]
22. Peshenko IV, Singh AK, Shichi H. Bovine eye 1-Cys peroxire-doxin: expression in *E. coli* and antioxidant properties. *J Ocul Pharmacol Ther*. 2001; 17:93–9. [PubMed: 11322641]
23. Wood ZA, Schroder E, Harris JR, Poole LB. Structure, mechanism and regulation of peroxiredoxins. *Trends Biochem Sci*. 2003; 28:32–40. [PubMed: 12517450]
24. Lyu MS, Rhee SG, Chae HZ, Lee TH, Adamson MC, Kang SW, et al. Genetic mapping of six mouse peroxiredoxin genes and fourteen peroxiredoxin related sequences. *Mamm Genome*. 1999; 10:1017–9. [PubMed: 10501973]
25. Fatma N, Singh DP, Shinohara T, Chylack LT Jr. Transcriptional regulation of the antioxidant protein 2 gene, a thiol-specific antioxidant, by lens epithelium-derived growth factor to protect cells from oxidative stress. *J Biol Chem*. 2001; 276:48899–907. [PubMed: 11677226]
26. Fatma N, Kubo E, Sen M, Agarwal N, Thoreson WB, Camras CB, et al. Peroxiredoxin 6 delivery attenuates TNF-alpha-and glutamate-induced retinal ganglion cell death by limiting ROS levels and maintaining Ca²⁺ homeostasis. *Brain Res*. 2008; 1233:63–78. [PubMed: 18694738]
27. Manevich Y, Fisher AB. Peroxiredoxin 6, a 1-Cys peroxiredoxin, functions in antioxidant defense and lung phospholipid metabolism. *Free Radic Biol Med*. 2005; 38:1422–32. [PubMed: 15890616]
28. Manevich Y, Sweitzer T, Pak JH, Feinstein SI, Muzykantov V, Fisher AB. 1-Cys peroxiredoxin overexpression protects cells against phospholipid peroxidation-mediated membrane damage. *Proc Natl Acad Sci USA*. 2002; 99:11599–604. [PubMed: 12193653]
29. Chhunchha B, Fatma N, Bhargavan B, Kubo E, Kumar A, Singh DP. Specificity protein, Sp1-mediated increased expression of Prdx6 as a curcumin-induced antioxidant defense in lens epithelial cells against oxidative stress. *Cell Death Dis*. 2011; 2:e234. [PubMed: 22113199]
30. Fatma N, Singh P, Chhunchha B, Kubo E, Shinohara T, Bhargavan B, et al. Deficiency of Prdx6 in lens epithelial cells induces ER stress response-mediated impaired homeostasis and apoptosis. *Am J Physiol Cell Physiol*. 2011; 301:C954–67. [PubMed: 21677259]
31. Wang X, Phelan SA, Forsman-Semb K, Taylor EF, Petros C, Brown A, et al. Mice with targeted mutation of peroxiredoxin 6 develop normally but are susceptible to oxidative stress. *J Biol Chem*. 2003; 278:25179–90. [PubMed: 12732627]
32. Gallagher BM, Phelan SA. Investigating transcriptional regulation of Prdx6 in mouse liver cells. *Free Radic Biol Med*. 2007; 42:1270–7. [PubMed: 17382207]
33. Roede JR, Stewart BJ, Petersen DR. Decreased expression of peroxiredoxin 6 in a mouse model of ethanol consumption. *Free Radic Biol Med*. 2008; 45:1551–8. [PubMed: 18852041]
34. Kubo E, Singh DP, Fatma N, Akagi Y. TAT-mediated peroxiredoxin 5 and 6 protein transduction protects against high-glucose-induced cytotoxicity in retinal pericytes. *Life Sci*. 2009; 84:857–64. [PubMed: 19351539]
35. Kubo E, Hasanova N, Tanaka Y, Fatma N, Takamura Y, Singh DP, et al. Protein expression profiling of lens epithelial cells from Prdx6-depleted mice and their vulnerability to UV radiation exposure. *Am J Physiol Cell Physiol*. 2010; 298:C342–54. [PubMed: 19889963]
36. Woo HA, Kang SW, Kim HK, Yang KS, Chae HZ, Rhee SG. Reversible oxidation of the active site cysteine of peroxiredoxins to cysteine sulfinic acid: immunoblot detection with antibodies specific for the hyperoxidized cysteine-containing sequence. *J Biol Chem*. 2003; 278:47361–4. [PubMed: 14559909]
37. Rhee SG, Chae HZ, Kim K. Peroxiredoxins: a historical overview and speculative preview of novel mechanisms and emerging concepts in cell signaling. *Free Rad Biol Med*. 2005; 38:1543–52. [PubMed: 15917183]
38. Schröder E, Littlechild JA, Lebedev AA, Errington N, Vagin AA, Isupov MN. Crystal structure of decameric 2-Cys peroxiredoxin from human erythrocytes at 1.7 Å resolution. *Structure*. 2000; 8:605–15. [PubMed: 10873855]
39. Hofmann B, Hecht HJ, Flohé L. Peroxiredoxins. *Biol Chem*. 2002; 383:347–64. [PubMed: 12033427]

40. Alphey MS, Bond CS, Tetaud E, Fairlamb AH, Hunter WN. The structure of reduced tryparedoxin peroxidase reveals a decamer and insight into reactivity of 2Cys-peroxiredoxins. *J Mol Biol.* 2000; 300:903–16. [PubMed: 10891277]
41. Wood ZA, Poole LB, Hantgan RR, Karplus PA. Dimers to doughnuts: redox-sensitive oligomerization of 2-cysteine peroxiredoxins. *Biochemistry.* 2002; 41:5493–504. [PubMed: 11969410]
42. Woo HA, Chae HZ, Hwang SC, Yang KS, Kang SW, Kim K, et al. Reversing the inactivation of peroxiredoxins caused by cysteine sulfinic acid formation. *Science.* 2003; 300:653–6. [PubMed: 12714748]
43. Rabilloud T, Heller M, Gasnier F, Lucche S, Rey C, Aebersold R, et al. Proteomics analysis of cellular response to oxidative stress: evidence for in vivo overoxidation of peroxiredoxins at their active site. *J Biol Chem.* 2002; 277:19396–401. [PubMed: 11904290]
44. Yang KS, Kang SW, Woo HA, Hwang SC, Chae HZ, Kim K, et al. Inactivation of human peroxiredoxin I during catalysis as the result of the oxidation of the catalytic site cysteine to cysteine-sulfinic acid. *J Biol Chem.* 2002; 277:38029–36. [PubMed: 12161445]
45. Wagner E, Lucche S, Penna L, Chevillet M, Van Dorsselaer A, Leize-Wagner E, et al. A method for detection of overoxidation of cysteines: peroxiredoxins are oxidized in vivo at the active-site cysteine during oxidative stress. *Biochem J.* 2002; 366:777–85. [PubMed: 12059788]
46. Kim SY, Jo HY, Kim MH, Cha YY, Choi SW, Shim JH, et al. H₂O₂-dependent hyperoxidation of peroxiredoxin 6 (Prdx6) plays a role in cellular toxicity via up-regulation of iPLA2 activity. *J Biol Chem.* 2008; 283:33563–8. [PubMed: 18826942]
47. Hasanova N, Kubo E, Kumamoto Y, Takamura Y, Akagi Y. Age-related cataracts and Prdx6: correlation between severity of lens opacity, age and the level of Prdx6 expression. *Br J Ophthalmol.* 2009; 93:1081–4. [PubMed: 19429582]
48. Becker-Hapak M, McAllister SS, Dowdy SF. TAT-mediated protein transduction into mammalian cells. *Methods.* 2001; 24:247–56. [PubMed: 11403574]
49. Mann DA, Frankel AD. Endocytosis and targeting of exogenous HIV-1 Tat protein. *EMBO J.* 1991; 10:1733–9. [PubMed: 2050110]
50. Nagahara H, Vocero-Akbani AM, Snyder EL, Ho A, Latham DG, Lissy NA, et al. Transduction of full-length TAT fusion proteins into mammalian cells: TAT-p27Kip1 induces cell migration. *Nat Med.* 1998; 4:1449–52. [PubMed: 9846587]
51. Rusnati M, Coltrini D, Oreste P, Zoppetti G, Albini A, Noonan D, et al. Interaction of HIV-1 Tat protein with heparin: role of the backbone structure, sulfation, and size. *J Biol Chem.* 1997; 272:11313–20. [PubMed: 9111037]
52. Kubo E, Fatma N, Sharma P, Shinohara T, Chylack LT Jr, Singh DP. Transactivation of involucrin, a marker of differentiation in keratinocyte, by lens epithelium-derived growth factor (LEDGF). *J Mol Biol.* 2002; 320:1053–63. [PubMed: 12126624]
53. Kubo E, Singh DP, Fatma N, Shinohara T, Zelenka P, Reddy VN, et al. Cellular distribution of lens epithelium-derived growth factor (LEDGF) in the rat eye: loss of LEDGF from nuclei of differentiating cells. *Histochem Cell Biol.* 2003; 119:289–99. [PubMed: 12692670]
54. Fawell S, Seery J, Daikh Y, Moore C, Chen LL, Pepinsky B, et al. Tat-mediated delivery of heterologous proteins into cells. *Proc Natl Acad Sci USA.* 1994; 91:664–8. [PubMed: 8290579]
55. Frankel AD, Pabo CO. Cellular uptake of the tat protein from human immunodeficiency virus. *Cell.* 1988; 55:1189–93. [PubMed: 2849510]
56. Kubo E, Singh DP, Akagi Y. Gene expression profiling of diabetic and galactosaemic cataractous rat lens by microarray analysis. *Diabetologia.* 2005; 48:790–8. [PubMed: 15761720]
57. Kubo E, Urakami T, Fatma N, Akagi Y, Singh DP. Polyol pathway-dependent osmotic and oxidative stresses in aldose reductase-mediated apoptosis in human lens epithelial cells: role of AOP2. *Biochem Biophys Res Commun.* 2004; 314:1050–6. [PubMed: 14751239]
58. Reddy GB, Bhat KS. Protection against UV-B inactivation (in vitro) of rat lens enzymes by natural antioxidants. *Mol Cell Biochem.* 1999; 194:41–5. [PubMed: 10391122]
59. Spector A. Oxidative stress-induced cataract: mechanism of action. *FASEB J.* 1995; 9:1173–82. [PubMed: 7672510]

60. Kubo E, Maekawa K, Tanimoto T, Fujisawa S, Akagi Y. Biochemical and morphological changes during development of sugar cataract in Otsuka Long-Evans Tokushima Fatty (OLETF) rat. *Exp Eye Res.* 2001; 73:375–81. [PubMed: 11520112]
61. Kubo E, Miyoshi N, Fukuda M, Akagi Y. Cataract formation through polyol pathway is associated with free radical production. *Exp Eye Res.* 1999; 68:457–64. [PubMed: 10192803]
62. Boscia F, Grattagliano I, Vendemiale G, Micelli-Ferrari T, Altomare E. Protein oxidation and lens opacity in humans. *Invest Ophthalmol Vis Sci.* 2000; 41:2461–5. [PubMed: 10937554]
63. McCormick JP, Fischer JR, Pachlatko JP, Eisenstark A. Characterization of a cell-lethal product from the photooxidation of tryptophan: hydrogen peroxide. *Science.* 1976; 191:468–9. [PubMed: 1108203]
64. Walker GC. Inducible DNA repair systems. *Annu Rev Biochem.* 1985; 54:425–57. [PubMed: 3896123]
65. Hightower KR. The role of the lens epithelium in development of UV cataract. *Curr Eye Res.* 1995; 14:71–8. [PubMed: 7720407]
66. Sachsenmaier C, Radler-Pohl A, Zinck R, Nordheim A, Herrlich P, Rahmsdorf HJ. Involvement of growth factor receptors in the mammalian UVC response. *Cell.* 1994; 78:963–72. [PubMed: 7923365]
67. Mai S, Stein B, van den Berg S, Kaina B, Lucke-Huhle C, Ponta H, et al. Mechanisms of the ultraviolet light response in mammalian cells. *J Cell Sci.* 1989; 94(Pt 4):609–15. [PubMed: 2698396]
68. Devary Y, Gottlieb RA, Smeal T, Karin M. The mammalian ultraviolet response is triggered by activation of Src tyrosine kinases. *Cell.* 1992; 71:1081–91. [PubMed: 1473146]
69. Stein B, Rahmsdorf HJ, Steffen A, Litfin M, Herrlich P. UV-induced DNA damage is an intermediate step in UV-induced expression of human immunodeficiency virus type 1, collagenase, c-fos, and metallothionein. *Mol Cell Biol.* 1989; 9:5169–81. [PubMed: 2557547]
70. Devary Y, Rosette C, DiDonato JA, Karin M. NF-kappa B activation by ultraviolet light not dependent on a nuclear signal. *Science.* 1993; 261:1442–5. [PubMed: 8367725]
71. Devary Y, Gottlieb RA, Lau LF, Karin M. Rapid and preferential activation of the c-jun gene during the mammalian UV response. *Mol Cell Biol.* 1991; 11:2804–11. [PubMed: 1901948]
72. Ayala M, Strid H, Jacobsson U, Soderberg PG. p53 expression and apoptosis in the lens after ultraviolet radiation exposure. *Invest Ophthalmol Vis Sci.* 2007; 48:4187–91. [PubMed: 17724205]
73. Ji Y, Cai L, Zheng T, Ye H, Rong X, Rao J, et al. The mechanism of UV-B irradiation induced-apoptosis in cataract. *Mol Cell Biochem.* 2015; 401:87–95. [PubMed: 25445170]
74. Cai SR, Xu G, Becker-Hapak M, Ma M, Dowdy SF, McLeod HL. The kinetics and tissue distribution of protein transduction in mice. *Eur J Pharm Sci.* 2006; 27:311–9. [PubMed: 16376528]

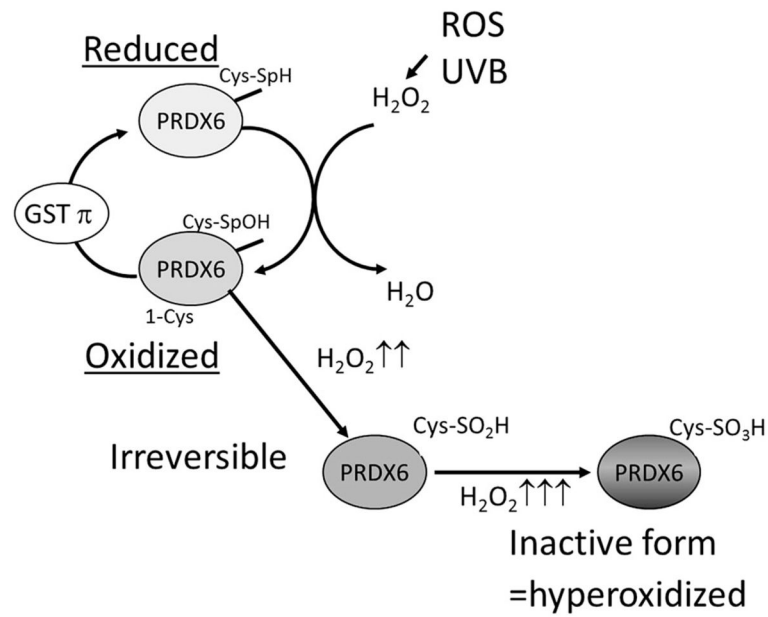


Fig. 1. Illustration of the mechanism of redox regulation by perox-iredoxin 6 (*Prdx6*). *Prdx6* detoxifies and controls intracellular levels of reactive oxidative species (*ROS*), providing cytoprotection by maintaining survival signaling. The active site cysteine (Cys47) is oxidized to cysteine sulfenic acid (Cys47-SOH) by hydrogen peroxide (H_2O_2). However, the resulting Cys47-SOH cannot form a disulfide bond because no other Cys-SH residues are present nearby. Cys47-SOH can be reduced by nonphysiologic thiols. Occasionally, the sulfenic intermediate is hyperoxidized to sulfinic ($Cys-SO_2H$) or sulfonic ($Cys-SO_3H$) acid, inactivating its peroxidase activity. *GST* Glutathione-S-transferase, *UV-B* ultraviolet B

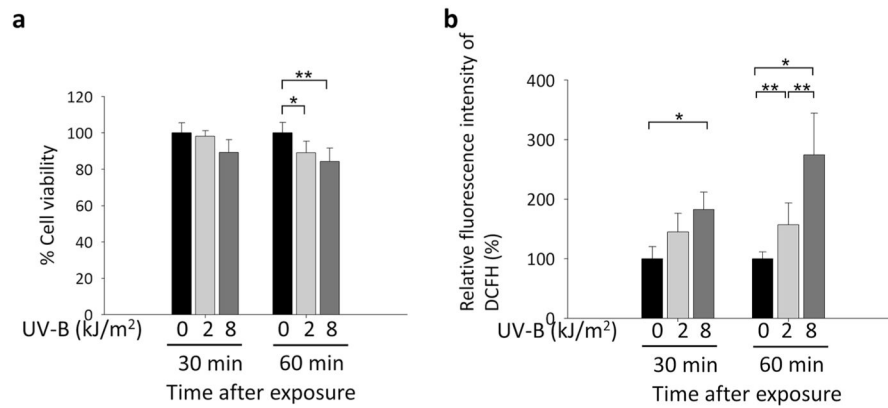


Fig. 2. Effects of UV-B exposure on cell viability and ROS levels in cultured human lens epithelial cells (hLECs). **a** Effects of 0, 2.0, or 8.0 kJ/m² UV-B treatment for 30 and 60 min on cell viability, as detected by the MTS assay (* $P < 0.05$, ** $P < 0.02$). **b** Effects of treatment with 0, 2.0, or 8.0 kJ/m² UV-B on ROS of hLECs for 30 and 60 min, as detected by H₂DCFH-DA assays (* $P < 0.004$, ** $P < 0.03$). Results are shown as the mean \pm standard deviation (SD) of three experiments. *Asterisks* denote significant differences. Section Assay for intracellular redox state and cell viability provides details on the assays

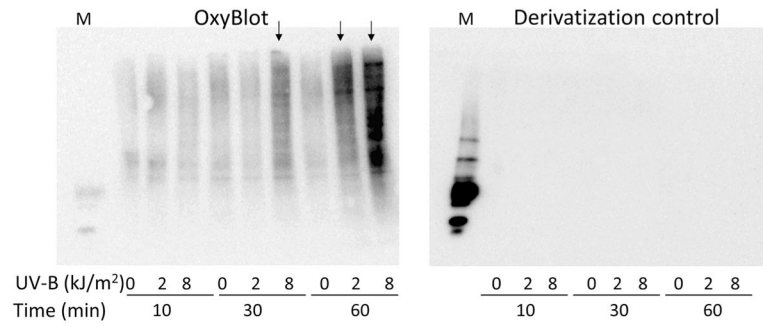


Fig. 3. Effects of UV-B exposure on carbonyl group formation on protein side chains in hLECs. hLECs were exposed to 0, 2.0, or 8.0 kJ/m² UV-B and processed for determination of protein oxidation using the OxyBlot Protein Oxidation Detection kit. To control for derivatization, proteins were not treated with DNP-hydrazine. *M* Marker

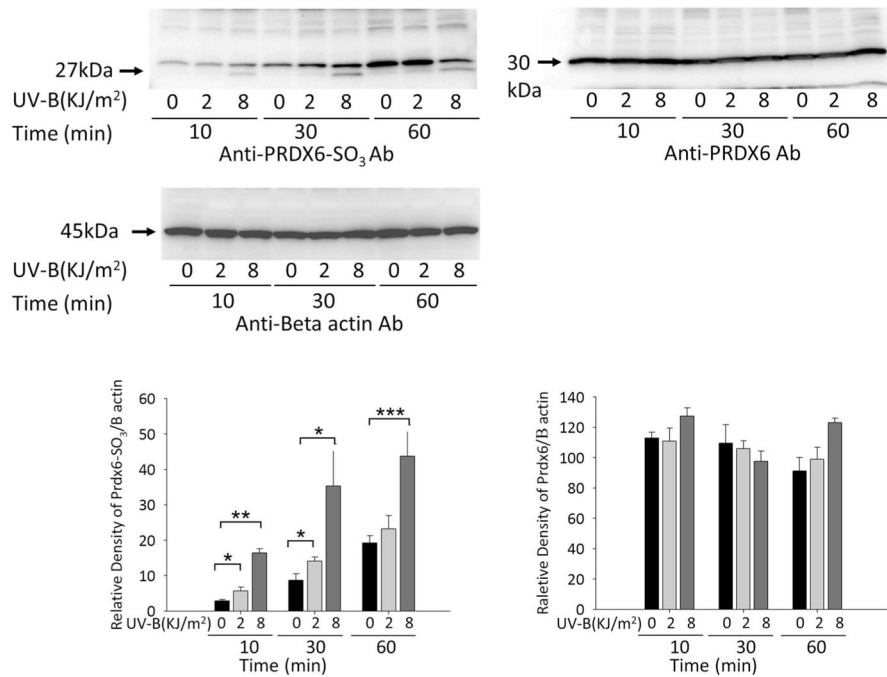
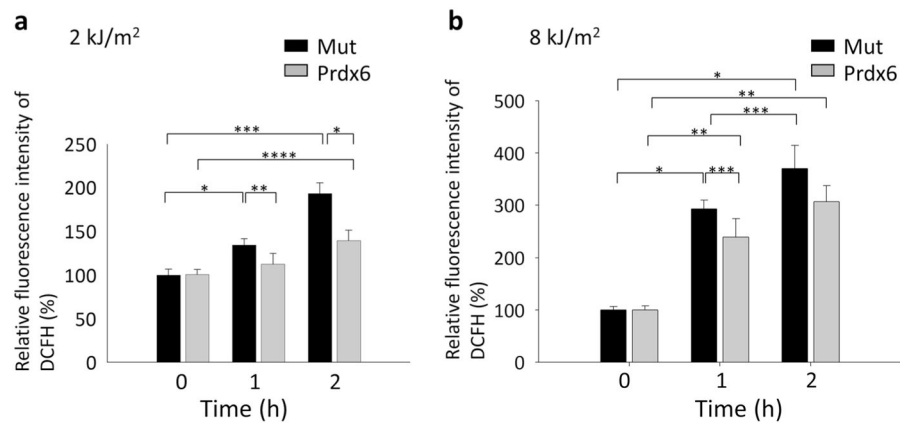
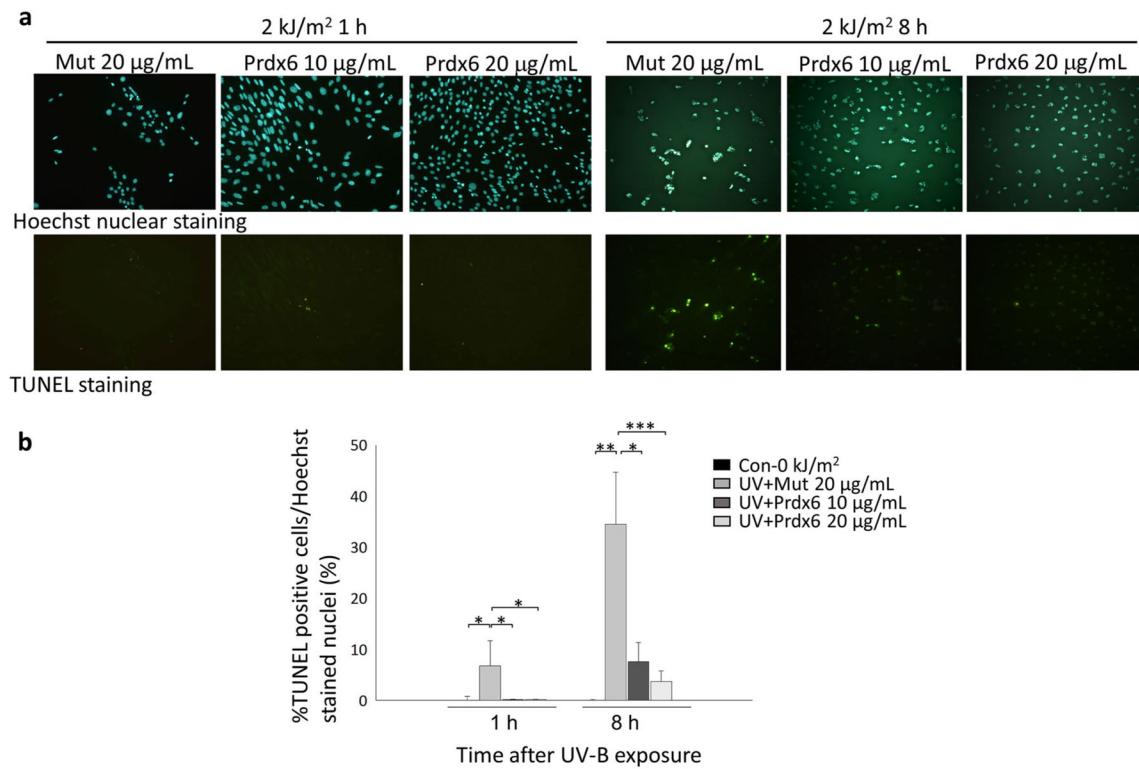


Fig. 4. Effects of UV-B exposure on hyperoxidized Prdx6 (*Prdx6-SO₃*) expression by cultured hLECs. Cells were exposed to 0, 2.0, and 8.0 kJ/m² UV-B and processed for protein blotting with antibody (*Ab*) to hyperoxidized Prdx6 (*Prdx6-SO₃*). *Prdx6-SO₃* was detected as 27- and 30-kDa bands. Results are shown as the mean ± SD of three experiments. *Asterisks* denote significant differences at **P* < 0.02, ***P* < 0.0001, and ****P* < 0.005

**Fig. 5.**

Treatment with the exogenous recombinant protein TAT-HA-Prdx6 (for details on its construction, see section Prokaryotic expression of recombinant Prdx6 protein) attenuated UV-B-induced generation of ROS. hLECs were treated with 10 $\mu\text{g/mL}$ TAT-HA-Prdx6 or TAT-HA-Prdx6 mutated at the active site (*Mut*) as the negative control, exposed to 2.0 (**a**) or 8.0 (**b**) kJ/m^2 UV-B for 1 and 2 h, and processed for quantitation of ROS levels using the H2-DCF-DA dye at excitation and emission wavelengths of 485 nm and 530 nm, respectively. **a** Extrinsic supply of TAT-HA-Prdx6 significantly reduced ROS levels after 1 and 2 h of exposure to 2.0 kJ/m^2 UV-B radiation ($*P < 0.0005$, $**P < 0.02$, $***P < 0.00002$, $****P < 0.003$). **b** Extrinsic supply of TAT-HA-Prdx6 significantly reduced ROS levels after 1 h of exposure to 8.0 kJ/m^2 UV-B radiation ($*P < 0.00002$, $**P < 0.0003$, $***P < 0.035$). Results are shown as the mean \pm SD of three experiments. *Asterisks* denote significant differences

**Fig. 6.**

Effect of TAT-HA-Prdx6 on UV-B-induced apoptosis of hLECs. hLECs were exposed to 0 [control (*Con*)] or 2.0 kJ/m² UV-B, and the percentage of apoptotic cells was determined by TUNEL assays after 1 and 8 h (for details on the assay, see section Apoptosis assay). **a** Representative photomicrograph of TUNEL staining. **b** Histograms showing the relative percentage of TUNEL-positive cells per Hoechst-stained nuclei. The addition of 10 and 20 µg/mL TAT-HA-Prdx6 significantly inhibited UV-B-induced apoptosis after 1 and 8 h (* $P < 0.01$, ** $P < 0.0001$, *** $P < 0.008$). Results are shown as the mean \pm SD of three experiments. *Asterisks* denote significant differences

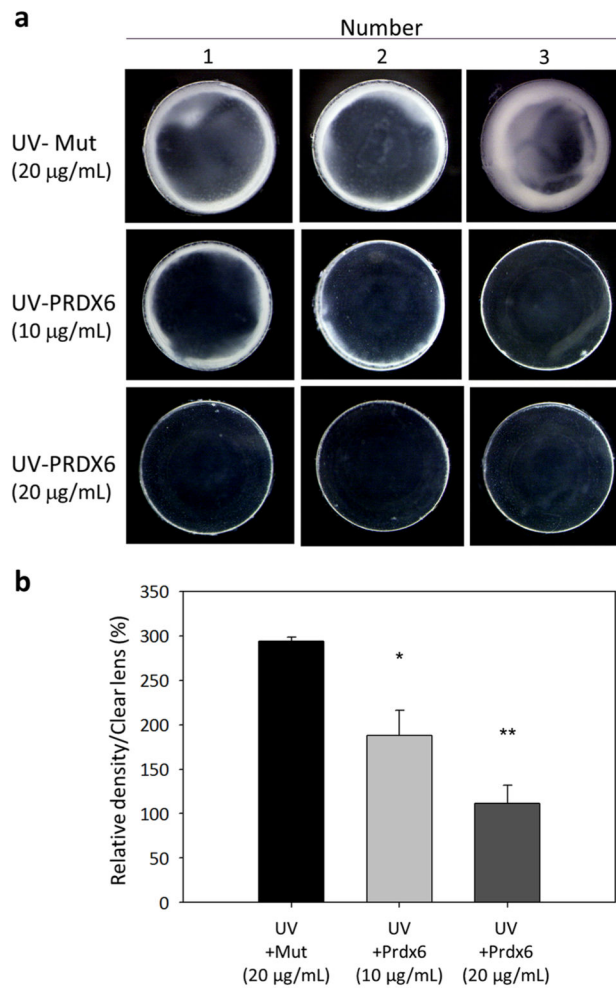


Fig. 7. Effects of TAT-HA-Prdx6 on the opacity of rat organ cultured lenses exposed to UV-B irradiation. Fifteen lenses from 12-week-old rats were organ-cultured for 24 h in Medium 199 containing 10 or 20 $\mu\text{g}/\text{mL}$ TAT-HA-Prdx6 ($n = 5$ per group) or 20 $\mu\text{g}/\text{mL}$ TAT-HA-Prdx6 with a mutation (*Mut*) at the active site. The cells were irradiated with 6.0 kJ/m^2 UV-B. **a** Photographs of 3 lenses at 120 h after UV-B treatment, showing the degree of lens opacity. **b** Histograms showing the density of opacity. The addition of 10 and 20 $\mu\text{g}/\text{mL}$ TAT-HA-Prdx6 significantly reduced UV-B-induced lens opacity (* $P < 0.004$, ** $P < 0.0002$). Results are shown as the mean \pm SD of three experiments. Asterisks denote significant differences